Environmental Science and Pollution Research (2022) 29:27421–27429
https://doi.org/10.1007/s11356-021-17899-0

RESEARCH ARTICLE

Mechanically activated calcium carbonate and zero-valent iron composites for one-step treatment of multiple pollutants

Yanhui Hu[1] · Weijian Gu[1] · Huimin Hu[1] · Xuewei Li[2] · Qiwu Zhang[1]

Received: 16 May 2021 / Accepted: 29 November 2021 / Published online: 4 January 2022

Abstract

The growing presences of conventional and emerging contaminants make the wastewater treatment increasingly difficult and expensive on a global scale. ZVI tends to be an expectable material for the detoxification of some difficult contaminants such as chlorinated solvents and nitroaromatics. In this work, together use with calcium carbonate ($CaCO_3$), which serves as a green supporter to ZVI and also direct participant toward the purification process, has been carried out by cogrinding to give a synergistic effect, particularly for treating multiple pollutants including both inorganic and organic compositions. Based on a set of analytical methods of XRD, FTIR, SEM, XPS, and other test methods, the activation mechanism of the ball milling process and the removal performances of the prepared composites were examined. The results prove that the mechanically activated calcium carbonate and ZVI composite samples exhibited extremely high removal capacity on a variety of pollutants contaminated water. The decolorization of azo dyes is mainly attributed to the breaking of chromogenic functional group nitrogen and nitrogen double bonds, and the removal mechanism of aromatic series occurs through a hydrogenation substitution reaction. As to the inorganic pollutant removals, besides the efficient heavy metal ion precipitations, phosphate and fluoride ions are co-precipitated through the formation of fluorapatite to achieve a simultaneous and synergistic removal effect. Under the optimal reaction conditions, the concentration of PO_4^{3-} is reduced from 250 to 0 mg/L, and that of F^- is reduced from 51.07 to 1.20 mg/L. The prepared composite sample of ZVI rand calcium carbonate allowed simultaneous removals of both inorganic and organic pollutants, simplifying the remediation process of complicated multiple contaminations.

Keywords Zero-valent iron · Calcium carbonate · Mechanical activation · Multicomponent pollutant

Introduction

As an agent to treat polluted water, zero-valent iron (ZVI) has the advantages of high reduction potential and fast reaction speed and has received intensive attention in the field of environmental remediation (Yang and Lee. 2005; Fu et al. 2014; Duan et al. 2015; Lawrinenko et al. 2016). Among various basic researches, $NaBH_4$ aqueous solution is usually used to synthesize ZVI by the reduction of iron salts. In this way, nanosized particles of ZVI as NZVI aggregate easily and measurements have to be taken to maintain high reactivity by using a protecting coating or dispersing carrier, such as clay (Sheng et al. 2014), graphene (Jabeen et al. 2011), carbon nanotubes (CNTs) (Vilardi et al. 2018), activated carbon (AC) (Xu et al. 2014), and so on (Chatterjee et al. 2010).

Another method to prepare ZVI by size reduction using a mechanical ball milling has attracted a lot of attention because of its easy operation and good industrialization prospects (Gong et al. 2018; Yang et al. 2019). Because of metal malleability, it is not easy to obtain fine particles by ball milling iron itself, and efforts are required to obtain fine powders to give high reactivity. Co-grinding iron powders with additives may represent a technologically feasible means of simultaneously achieving facile preparation and viable preservation. Furthermore, the additive may be capable of treating some different pollutants to which ZVI does not work efficiently.

Responsible Editor: Weiming Zhang

✉ Xuewei Li
lixuewei126@126.com

✉ Qiwu Zhang
zhangqw@whut.edu.cn

[1] School of Resources and Environmental Engineering, Wuhan University of Technology, Luoshi Road 122, Wuhan 430070, Hubei, China

[2] Ganjiang Innovation Academy, Chinese Academy of Sciences, Jiangxi 341109, China

$CaCO_3$ is the main composition of abundantly available calcite mineral around the world (Li et al. 2017), with obvious advantages of low price, high chemical purity, stability, and high whiteness. It is widely used in various industrial fields such as fillers in papermaking, plastics, rubber, and coating powders. Compared with $Ca(OH)_2$, $CaCO_3$ itself is too stable to be used directly for a chemical precipitation of heavy metals, although the use of $CaCO_3$ as an adsorbent for metal removal has been widely studied. $Ca(OH)_2$ is produced from $CaCO_3$ by thermal decomposition to give high reactivity used in the alkali precipitation treatment. It is difficult to use calcite to react with metal ions chemically at the natural state. Possible transformation of calcite to raise its reactivity high enough close to calcium hydroxide would be interesting and applicable for environmental purification including heavy metal removals. Mechanical activation is well known to be able to raise reactivity of target sample and even trigger a kind of direct reaction as mechanochemical one (Beyer and Clausen-Schaumann 2005; James et al. 2011; Balaz et al. 2013; Huot et al. 2013). Therefore, we proposed mechanical activation as an alternative to raise the reactivity of $CaCO_3$ near to that of $Ca(OH)_2$ to treat heavy metal wastewaters through similar precipitation reaction rather than a physical adsorption. We conducted wet grinding of $CaCO_3$ in the solutions containing copper, iron, and lead cations and confirmed the precipitation reactions at nearly stoichiometric ratios resulting from the enhanced reactivity (Hu et al. 2017, 2019; Li et al. 2018).

$CaCO_3$ was selected as the additive to prepare composite sample with ZVI, and the effectiveness of ZVI and $CaCO_3$ composite in the treatment of hexavalent chromium was confirmed (Gu et al. 2019). The purpose of this work is to explore the possible synergistic effects of ZVI and $CaCO_3$ in the prepared composite sample to allow one-step removal of multicomponent pollutants including inorganic cations and anions, as well as organics. In addition to the possible removal of cationic metals, the first part of this study was to use only the activated $CaCO_3$ to remove phosphate and fluoride anions. As the second part, the composite was used to treat azo dye wastewater such as acid red 73, as well as chlorobenzene and nitrobenzene. Finally, a simulated wastewater with various heavy metals including Cu, Pb, Zn, Ni, Cd, Cr(VI), As(V), anions of PO_4^{3-}, F^-, and acid red 73, chlorobenzene, and nitrobenzene was prepared, and removal performances were examined by using the ZVI and $CaCO_3$ composite.

Experimental section

Material preparation

Iron powder (Fe^0), calcium carbonate ($CaCO_3$), potassium dihydrogen phosphate (KH_2PO_4), sodium fluoride (NaF), potassium dichromate ($K_2Cr_2O_7$), sodium hydrogen arsenate heptahydrate ($Na_2HAsO_47H_2O$), copper sulfate pentahydrate ($CuSO_45H_2O$), zinc sulfate heptahydrate ($ZnSO_47H_2O$), nickel sulfate hexahydrate ($NiSO_46H_2O$), cadmium sulfate 8/3 hydrate ($CdSO_48/3H_2O$), lead nitrate ($Pb(NO_3)_2$), chlorobenzene (C_6H_5Cl), nitrobenzene ($C_6H_5NO_2$), and acid red 73 ($C_{22}H_{14}N_4Na_2O_7S_2$) were all purchased from Sinopharm Chemical Industry. All the reagents were analytically pure and used without further treatment. Ultrapure water was used to prepare solutions containing every contaminant at different initial concentrations: 200 mg/L acid red, 250 mg/L phosphate, 51.07 mg/L fluoride, all the other heavy metals and chlorobenzene, nitrobenzene of 10 mg/L, respectively.

The activation operation of zero-valent iron was carried out by a simple ball milling with a Pulverisette-7 planetary ball mill. A certain amount of the iron powder and $CaCO_3$(total 2 g) were put into a zirconia grinding pot (45 cm^3), together with grinding media (zirconia ball in diameter of 15 mm) and subjected to grinding for 8 h at 500 rpm except for detailed description in a batch step with all the sample recovered each time for characterizations.

Characterizations

An X-ray diffractometer (RU-200B/D/Max-RB, Rigaku, Japan) was used to identify phase existence in the samples before and after the grinding operation and after the removal of contaminants. Fourier transformed infrared (FTIR) (Nicolet6700, Thermo) spectra of the samples were measured over 4000–500 cm^{-1} using a KBr as a diluent. A thermogravimetric(TG) analysis (STA449F3, NETZSCH) was conducted in a nitrogen gas flow from 30 to 1400 ℃ at a heating rate of 10 ℃/min to reveal the difference of reaction products. A scanning electron microscope (JSM-IT300) was used for the observation of particle morphology. An X-ray photoelectron spectrometer (ESCALAB 250Xi) was used to investigate the changes in iron valence.

Removal experiments of multicomponent pollutants

The experiments of removing different types of pollutants by zero-valent iron samples after activation were carried out in a constant temperature (25 °C) water bath shaking tank (SHA-CG16-WS). A certain amount of the sample was placed in the prepared solutions containing target pollutants and shaken for 0.5–4 h.

The pH of samples in solutions were measured by a pH meter (METTLER TOLEDO FE20-FiveEasy™, Switzerland). The fluoride anion concentrations were determined potentiometrically using a fluoride ion-selective electrode (PXSJ-216F, China). The remaining concentrations of acid red 73, Cr(VI), and PO_4^{3-} in various solutions after removal

experiments were measured by a spectrometric method (Spectrophotometer UV mini-1240, Shimadzu Instruments, Japan) at 273 nm, 540 nm and 710 nm, respectively. Molybdenum blue colorimetric method was used to measure the arsenic concentration in filtrate at 880 nm (Orion Qquamate, Thermo Scientific, USA). The concentrations of all other heavy metal were measured using atomic absorption spectrometry (AAS: SHIMADZU AA-6880, Japan). The concentrations of chlorobenzene and nitrobenzene were measured by high-performance liquid chromatography (HPLC: 1260 Infinity, USA), with the chromatographic column of C18 (150 mm×5 mm, 5 μm), the column temperature at 25 °C, and methanol as mobile phases.

The removal percentage was calculated by the following (Eq. 1):

$$\eta(\%) = \left(c_0 - c_t\right)/c_0 \times 100\% \quad (1)$$

η (%) is the removal percentage of each pollutant; c_0 (mg/L) is the initial concentration of target pollutant; c_t (mg/L) is the concentration after the treatment.

Results and discussion

Simultaneous removals of phosphate and fluoride anions by using activated calcium carbonate

Calcium compounds of hydroxide or other soluble salts are usually used to remove these two anions. Raw $CaCO_3$ as an insoluble Ca source did not give high capacity, shown in Fig. 1, where the raw $CaCO_3$ and the 2 h ground $CaCO_3$ were compared at Ca/P/F ratio of 5/3/1 corresponding to the composition of fluoroapatite. The removal percentages of PO_4-P and F^- by using raw $CaCO_3$ were only 5.8% and 0.8%, respectively. Such low values indicate only surface adsorption of two anions on the raw $CaCO_3$ particles. On the other hand, by using activated $CaCO_3$, large increases in the removal percentages of PO_4-P and F^- are observed, reaching 73.8% and 59.2%, respectively with agitation time of 4 h. On the other hand, in cases of solutions with separate PO_4-P or F^- anion for comparison with the PO_4-P and F^- coexisting solution, the activated $CaCO_3$ gave relatively good removal performance (57%) for PO_4-P anion and poor efficiency (25%) for F^- anion. Removal of F^- anion by even using the activated $CaCO_3$ relied on the synergistic effect with PO_4-P anion.

The removal efficiencies of phosphate and fluoride are significantly enhanced by the mechanically activated $CaCO_3$, of which, as shown in S1, all the diffraction peaks had become almost unobservable, indicating that the regular crystalline structure of raw $CaCO_3$ was transformed into a nearly amorphous state under the action of mechanical force.

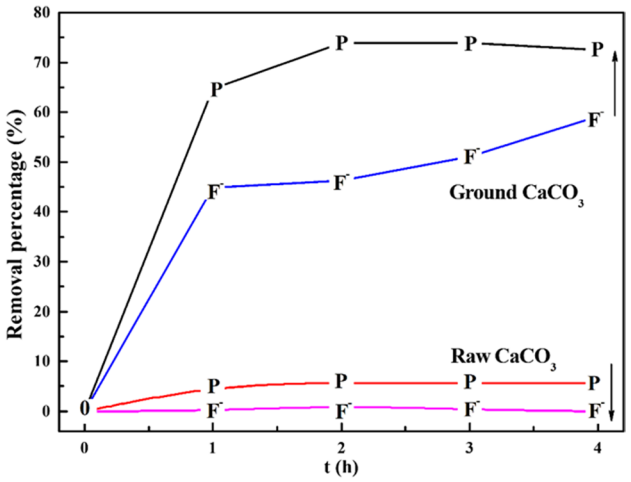

Fig. 1 Removal percentages of PO_4-P and F^- by using raw and activated $CaCO_3$ with Ca/P/F at 5:3:1

The solubility of calcium ion was enhanced in the presence of amorphous $CaCO_3$, contributing to the enhanced performances for two anion removals. Although the dissolved Ca^{2+} from ground $CaCO_3$ increased, it is still low compared with soluble calcium salts. The amount of $CaCO_3$ used at the exactly molar ratio for forming apatite was not enough for achieving complete removals of two anions.

The effect of the amount of the activated $CaCO_3$ on the removals of PO_4-P and F^- was investigated by fixing the molar ratio of P/F^- at 3:1, and the results are shown in Fig. 2. Increases in removal percentages of PO_4-P and F^- were clearly observed with increases in both agitating time and the amount of activated $CaCO_3$. Stirring the solution for 4 h and leaving the solution to stand for 12 h without further stirring gave satisfactory removal percentages close to 100% of both anions. With a specific molar ratio of Ca/P at 30:3 and stirring time at 3 h, the PO_4-P removal reached 100%. The removal rate of F^- at 4 h increased from 59 to 95% with the molar ratio of Ca/P increased from 5:3 to 50:3. Under the conditions of Ca/P/F at 30:3:1, stirring time of 4 h, the concentration of PO_4-P was reduced from 250 mg/L to 0 mg/L, and that of F^- reduced from 51.07 mg/L to 1.20 mg/L.

When calcium hydroxide is used to precipitate these anions, pH of the solution is usually increasing to a high alkaline range. However, in the case of using the activated $CaCO_3$, as shown in S2, changes with solution pH at different dosages of $CaCO_3$ were found in a very narrow neutral range from 6 to 8, indicating that the wastewater may be directly discharged without the need to monitor pH, a significant advantage for using $CaCO_3$ over $Ca(OH)_2$.

Figure 3 shows the XRD patterns of the precipitates generated from solutions of F^- alone, PO_4-P alone, and F^- and PO_4-P coexisting. It can be seen that only

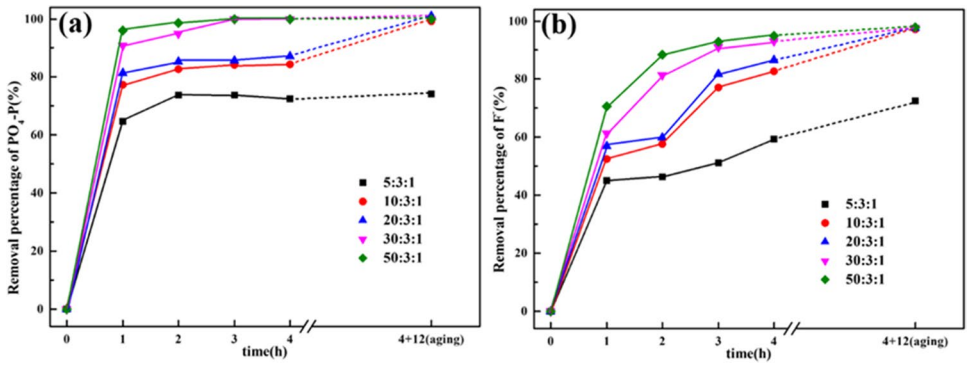

Fig. 2 Removal percentages of PO_4-P and F^- under different dosages of the activated $CaCO_3$

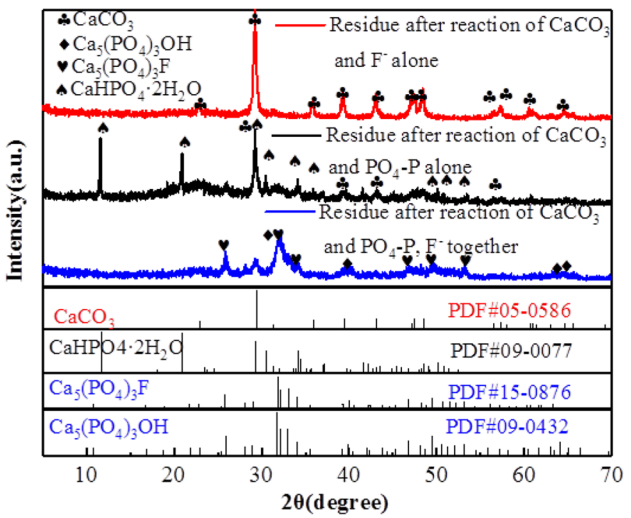

Fig. 3 XRD patterns of the precipitates generated by activated $CaCO_3$ from different solution compositions

the phase of $CaCO_3$ was found in the precipitate from F^--containing solution, indicating that no obvious reaction between $CaCO_3$ and fluoride occurred, corresponding to the very low removal percentage of F^- anion. A new phase of $CaHPO_4 2H_2O$ (brushite) (Mandel and Tas 2010) was observed in the precipitate from PO_4-P containing solution, and the peak intensity of $CaCO_3$ became much weaker than that from F^--containing solution, confirming the much consumption of $CaCO_3$ with phosphate anion to form the new phase. It is more important to note that the formation of new phases of $Ca_5(PO_4)_3F$ (fluoroapatite) and $Ca_5(PO_4)_3OH$ (hydroxyapatite) (Kong et al. 2020) in the precipitate from PO_4-P and F^- coexisting was detected, an indication of synergistic effect to form a new phase of fluoroapatite and therefore to contribute to the enhanced removal effects of both anions. From above, it is understood that Eqs. (2)~(4) as follows would occur in the process of treating PO_4-P and F^- wastewater by the activated $CaCO_3$.

$$5CaCO_3 + 3PO_4^{3-} + F^- = Ca_5(PO_4)_3F \downarrow + 5CO_3^{2-} \quad (2)$$

$$5CaCO_3 + 3PO_4^{3-} + 5H_2O = Ca_5(PO_4)_3OH \downarrow + 5CO_2 \uparrow + 9OH^- \quad (3)$$

$$CaCO_3 + PO_4^{3-} + 3H_2O = CaHPO_4 \cdot 2H_2O \downarrow + OH^- + CO_3^{2-} \quad (4)$$

SEM observations as shown in Fig. 4 demonstrated a clear change in morphologic feature and elemental compositions by EDS confirmed the phase compositions in agreement with the results in Fig. 3. The shape of the sample from F^--containing solution in (c) appeared in almost the same state of agglomerated particles as that of the amorphous calcium carbonate, suggesting a very weak reactivity of F^- present alone with the activated $CaCO_3$. The petal morphology of the sample in (b) was the typical feature of brushite reported in the literature (Toshima et al. 2018). Brushite phase of $CaHPO_4 2H_2O$ instead of $CaCO_3$ as the main phase confirmed the reaction pathway of Eq. (3) in the case of PO_4-P alone presence. In the case of PO_4-P and F^- coexisting shown in picture (a), cluster and rod-like structures, consistent with the morphology of the fluoro(hydroxy) apatite reported in the literature (Jioui et al. 2016; Wang et al. 2019) were clearly observed. Three different morphologic features reflected the different main phases exiting in the precipitating products, resulting from different reaction performances of $CaCO_3$ with three solutions containing different anions.

TG curves of the precipitates are shown in Fig. 5. The loss on ignition (LOI) at 600~800 °C was attributed to the thermal decomposition of $CaCO_3$ (Jeon and Kim 2019). The value of LOI is a reflection of the remaining amount of $CaCO_3$ in the sample, taken as an indicator of the reactivity with the anions compositions. When calcium carbonate was used to treat fluoride ions alone, the ignition loss of the precipitate after the reaction was 41.09% at 600–800 °C, which indicates that more than 93% of calcium carbonate remains in the precipitate. In other words, calcium carbonate has very low reactivity with fluoride

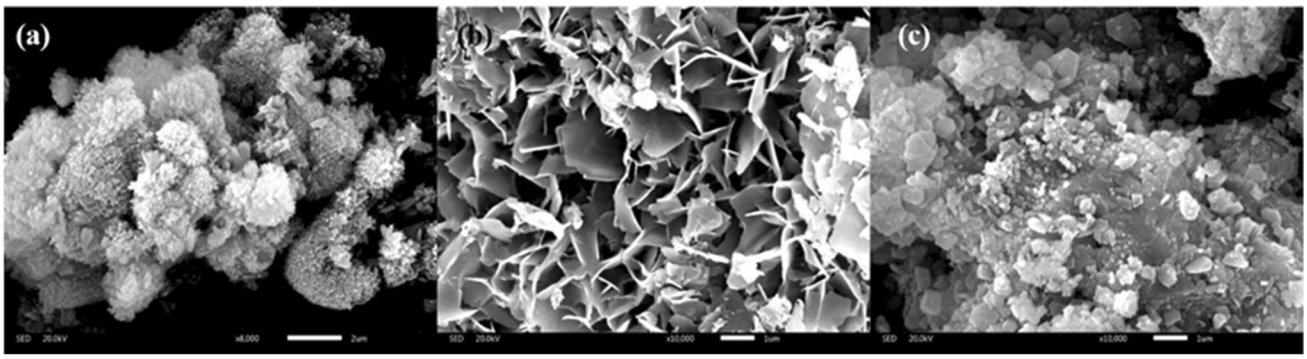

Fig. 4 SEM-EDS images of the precipitates from solutions of F^-, PO_4-P coexisting (**a**), PO_4-P alone (**b**), and F^- alone (**c**)

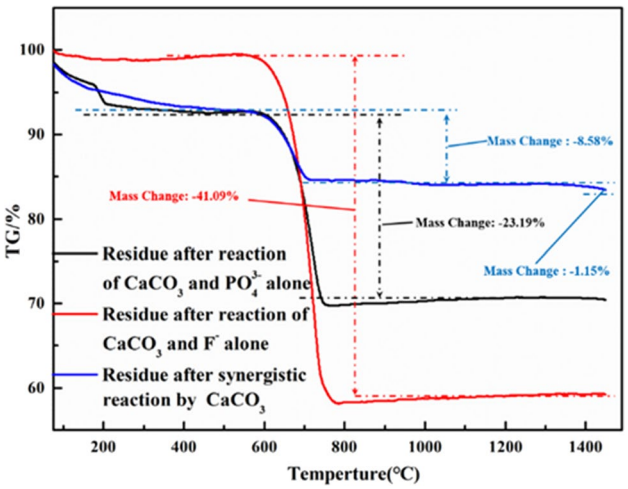

Fig. 5 TG curves of the precipitates under different conditions

ions alone. For the precipitate from PO_4-P containing solution, LOI of 23.19% demonstrated that the proportion of $CaCO_3$ in the precipitate was about 52%, with a large proportion of newly formed compound of calcium hydrogen phosphate dihydrate, which gave a certain mass loss even at temperature at 200 °C (Qin et al. 2018). And in the case of the solution containing fluoride and phosphate, the mass loss of 8.58% showed that less than 19% $CaCO_3$ existed in the precipitate, and most of $CaCO_3$ had transformed into new phases of apatite confirmed by XRD analysis. All the data from TG analysis confirmed again that the activated $CaCO_3$ presented much higher reactivity with PO_4-P and F^- together as compared to the case of these anions individually, based on a synergistic effect to form fluoroapatite. In addition, as to the information on the fluoride existence, the LOI at 1300~1400 °C may be attributed to a defluorination of fluoroapatite, which was observed only on the precipitate from PO_4-P and F^- coexisting (Hidouri et al. 2003).

Preparation of ZVI and $CaCO_3$ composite and subsequent treatment of organic wastewater

Water-soluble dyes with various compositions are major pollutants in textile dyeing industry wastewater and require adequate treatment. The application of nZVI on dye degradation has received wide attention in recent years due to the advantages of high reactivity, less toxicity, and good economic performance. The current processes for dye contaminant removal may involve complex phenomena including reduction, oxidation, sorption, and coprecipitation processes, which are further complicated under aerobic conditions related to oxygen intrusion. The focus of present work was to confirm the possibility of applying micron-sized ZVI at micron size prepared by cogrinding with $CaCO_3$ to treat the typical dye wastewater just in air, to offer a simple process and a product with good cost performance (Raman and Kanmani 2016; Xu et al. 2016).

As shown in Fig. 6a, zero-valent iron is round and uniform, and the particle size is maintained in the range of tens of microns, while the morphology of the zero-valent iron sample after individual ball milling shows great differences. As shown in Fig. 6b, the sample shows the evidence of heavy aggregation. The originally round and uniform spherical solids became flattened, and the fresh surface of the zero-valent iron after ball milling was densely packed in layers. The activity of zero-valent iron products is not increased, as shown in Fig. 7. The reason is that pure iron is soft and has good ductility. In the process of self-ball milling, zero-valent iron itself tends to be further flattened without evident breakdown. As a result of particle flattening and aggregation, the average particle size of the product becomes even larger instead.

In comparison, with the addition of a grinding aid of calcium carbonate, the morphology of the sample has been greatly changed. As shown in Fig. 6c and d , the addition of calcium carbonate during the ball milling process greatly improves the dispersibility of the final powder product, and

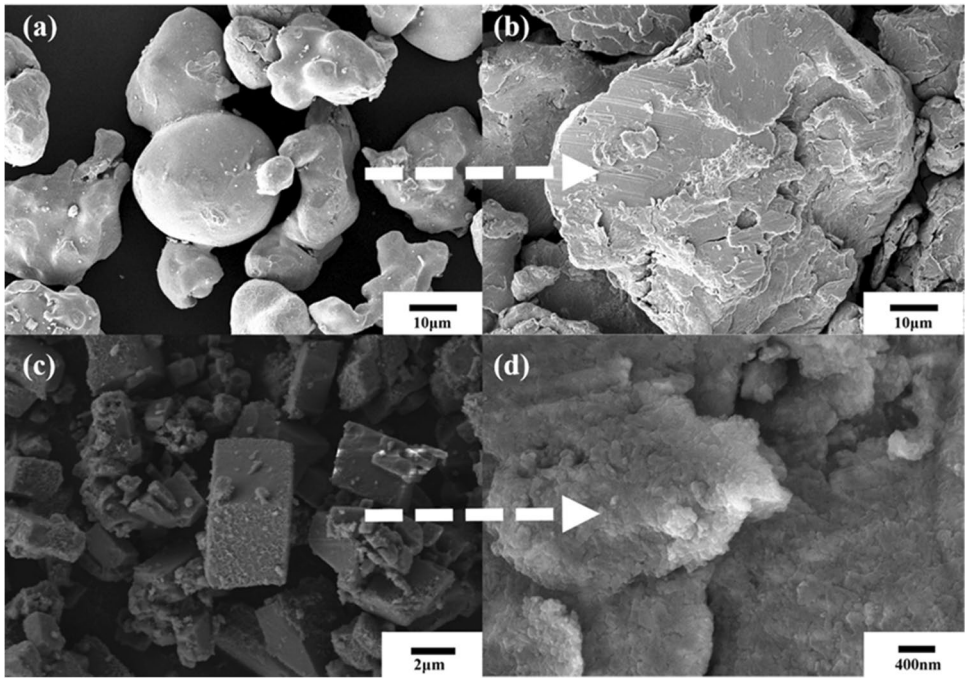

Fig. 6 SEM image: zero-valent iron as-is (**a**), ground zero-valent iron alone (**b**), calcium carbonate as-is (**c**), ground mixture of Fe and $CaCO_3$ (**d**)

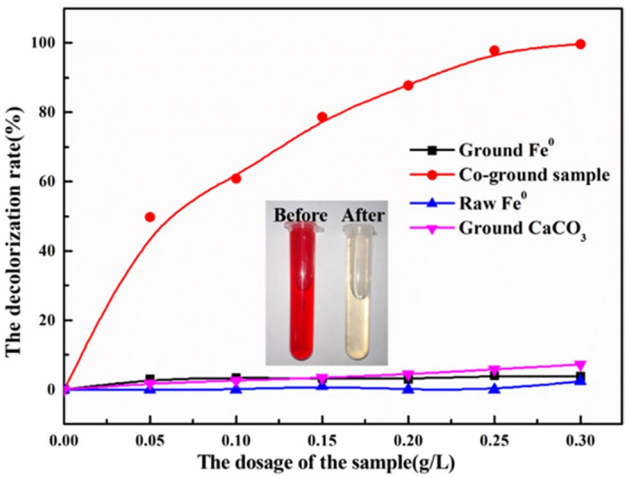

Fig. 7 Feasibility analysis of acid red 73 removal by mixed samples

the agglomerates disappear and are replaced by a zero-valent iron sample coated with calcium carbonate. The mixed sample presents a dense oolitic structural morphology. The hybrid activation by mechanical force can effectively alleviate the agglomeration of zero-valent iron during the ball milling process. The grinding aid of calcium carbonate forms a coating layer on the surface of the zero-valent iron to protect the fresh surface generated during the ball milling process. Besides the SEM observation of several particles, particle size distribution was also considered to assess the potential changes in particle size of the samples ground under different conditions and the results are shown in S3. Compared with starting iron powders, the ground sample gave a clear shifting of particle size to larger side, consistent with the SEM observation. When $CaCO_3$ was added for cogrinding, shifting of particle size to smaller side was obtained, indicating a breaking down effect. Different from the nanosized particles of nZVI from the solution method by $NaBH_4$ reduction, for example, the sample prepared by grinding remained in the range of micron size.

Decolorization of acid red sample was examined to evaluate the effect of the prepared ZVI sample, and Fig. 7 shows the comparison among four samples. With sample dosage up to 0.3 g/L, the samples of raw Fe^0, ground Fe^0, and ground $CaCO_3$ did not exhibit capacity for acid red removal. Cogrinding iron with $CaCO_3$ at same weight ratio could remove acid red efficiently and a complete decolorization was achieved at dosage of 0.3 g/L. As shown in S4, the decolorization reaction progressed very fast and ended up at 40 min. Fine particles usually give high reactivity, which would allow ZVI to be oxidized easily in air to form a passivation layer again on the surface to lose the high reactivity. The co-milling of zero-valent iron and calcium carbonate can maintain its high reactivity by avoiding the formation of passivation layer. It can be used as a reducing agent to break the azo double bond of the azo dye, so that the azo dye can be reduced and decolorized, although no mineralization has been obtained yet. Similar phenomena have been observed and reported to reduce hexavalent chromium.

Surface properties of the prepared ZVI sample were investigated by XPS analysis and information on element Fe only is shown in Fig. 8. Due to the $CaCO_3$ coating, the curves were very flattened with weak signals. Both divalent and trivalent states of iron were clearly observed, resulting

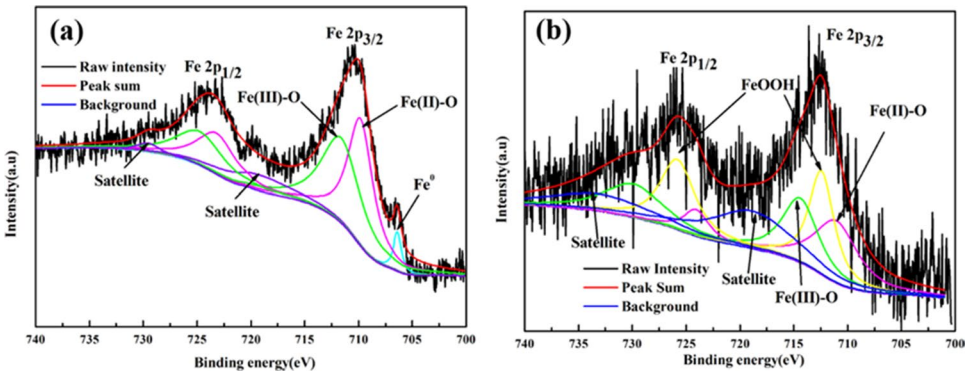

Fig. 8 XPS image comparison of the mixed sample and the residue after the reaction. **a** Mixed mechanically activated sample. **b** Mixed sample after reaction with Acid Red 73 residue

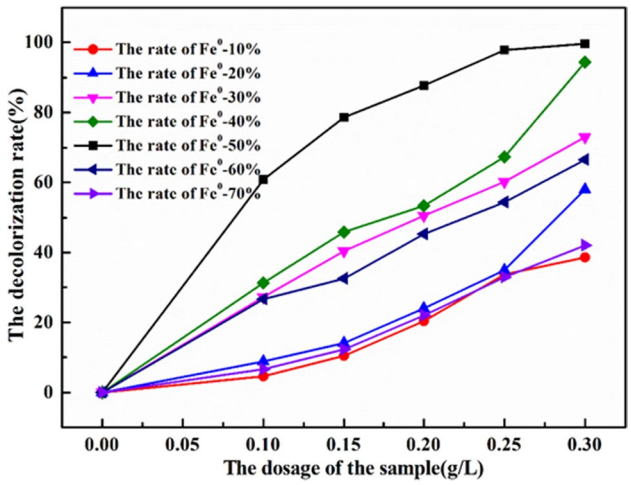

Fig. 9 Comparison of removal effect of acid red 73 under different proportions of zero-valent iron in mixed samples

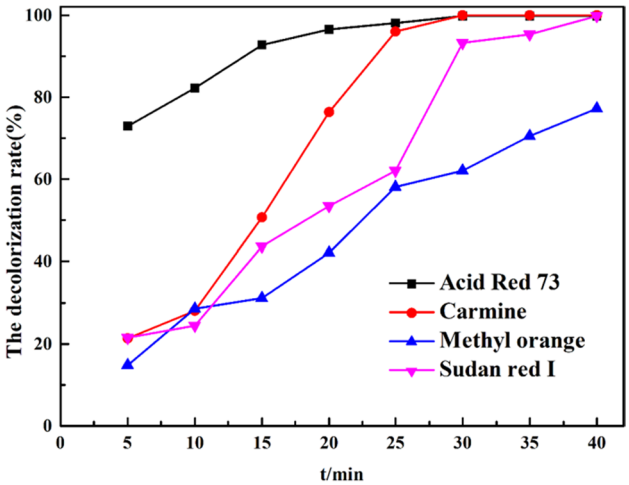

Fig. 10 Comparison of removal performances of different azo dyes

from the surface oxidization. It was worth of noting that a peak belonging to Fe^0 appeared in the spectrum of the prepared ZVI sample (Fig. 8a), and this peak was hardly to observe from the raw iron sample and ground sample without $CaCO_3$ addition during grinding operation. After treatment of acid red sample, the Fe^0 peak disappeared from the spectrum of the residual sample, suggesting that a reaction with the dye sample had consumed this composition. In other words, the key to using ZVI samples to treat contaminants was how to maintain the Fe^0 state and avoid oxide layers on the surface of the iron powder.

The performances of the prepared ZVI sample by cogrinding with $CaCO_3$ may be affected by grinding conditions including grinding time, running speed, etc. The weight ratio of iron to $CaCO_3$ was found to be important factor also. Figure 9 shows the changes in decolorization efficiency by the samples with different iron weight ratio in a range from a low 10% to a high 70%. All samples had a certain ability to decolorize dyes, however, large differences in this ability appeared, depending on the weight ratio of $CaCO_3$ added. When the content of zero valent iron in the mixed sample was 10% and 70%, the performance was low, and best performance of the composite sample was obtained when the content of zero valent iron was 50%. In other words, there exists an optimized adding amount of $CaCO_3$ for achieving both purposes of breaking down iron particles and coating the freshly formed active surfaces.

Besides Acid Red 73, several different azo dye samples were treated by the prepared ZVI sample and the results are shown in Fig. 10. Similar to Acid Red 73, Carmine and Sudan I were almost completely decolorized after 40 min of treatment, but the removal rate was not as fast as that of Acid Red 73 in the early stage. Decolorization of methyl orange reached around 80% at 40 min, not so efficiently as that of acid red 73, possibly due to less existence of N=N bonding in the structure. Variation in decolorization efficiency to some degree occurred with these four azo-dye samples and further investigation is required to understand the detailed reaction mechanism for each sample. ZVI and $CaCO_3$ composite sample worked well in general to break the N=N bonding in these azo dyes.

Pollutants of aromatic compounds are very difficult to deal with. Chlorobenzene and nitrobenzene were chosen as

examples and treatment by the prepared ZVI was performed. The dye sample with an initial concentration of 200 mg/L was almost completely decolorized at 40 min, while the aromatic samples with an initial concentration of 10 mg/L reached only about 50% removal efficiency after 120 min, as shown in Fig. 11. We are now continuing our study to monitor the grinding operation by adding different compounds to raise the reactivity of ZVI, aiming at achieving a high removal efficiency even for these typical aromatic pollutants.

With all these results, together with previous reports, we prepared a simulation waste solution: 100 ml distilled water containing 10 mg/L for Cu, Pb, Zn, Ni, Cd, Cr(VI), As(V), F^-, chlorobenzene and nitrobenzene; 50 mg/L for PO_4^{3-}; and 200 mg/L for Acid Red 73, respectively. With 1 g/L dosage of the ground ZVI and $CaCO_3$, removal performances for the multiple pollutants were summarized in Figure 12. The data indicated in general that the prepared sample enabled a one-step treatment of such multiple pollutants, supported by the nearly 100% removal efficiency of the target pollutants, although exception existed, particularly further effort is required to improve activity for removing aromatic group.

Besides the NVI particles prepared by solution methods, many publications have been available by grinding operation to raise the reactivity of ZVI through the modification of the particles by sulfidization, or cogrinding with some semiconductors to increase the electron transfer from ZVI to pollutants. The present work focused on the protecting effect of by cogrinding with $CaCO_3$ on the freshly formed active surface, so that the whole operation for sample handling could be conducted in the air without the need of using glovebox. The prepared sample maintained the reactivity for 1 week when stored in a typical plastic bag in air, indicating the very high applicable advantage for environmental issues. The ground $CaCO_3$ worked as

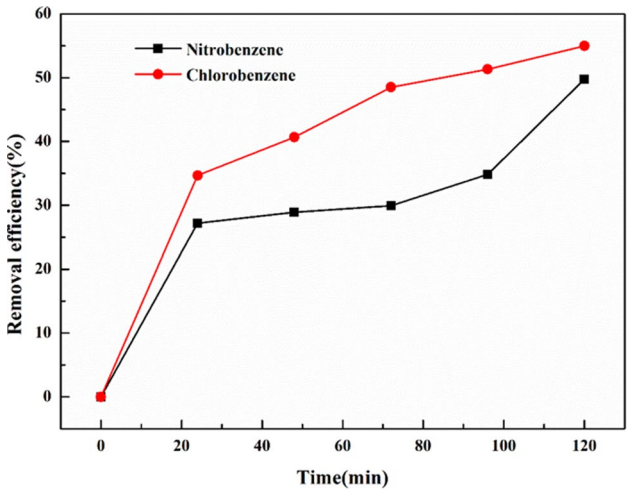

Fig. 11 Changes in removal efficiency of nitrobenzene and chlorobenzene with time

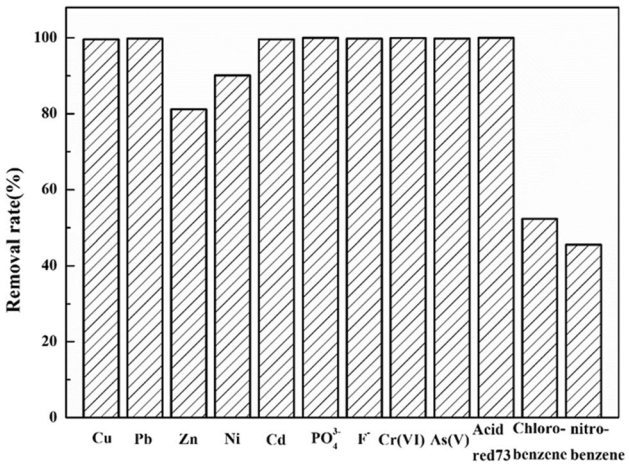

Fig. 12 Removals of multiple pollutants with the prepared sample

not only for ZVI protection but also very active sample directly for the purifications of other pollutants, particularly those not applicable by ZVI, giving the preparation method and the sample another advantage.

Conclusion

Mechanical grinding of iron powders alone could not enhance its reactivity because it was very difficult to break down the particles and the new surfaces of part broken ones were covered with passivation layer without proper protection. Such problems could be imply overcome by cogrinding with $CaCO_3$, to allow the ground samples as active ZVI to demonstrate excellent removal performances for Cr(VI), As(V), azo dyes and even observable capacity for treating chlorobenzene and nitrobenzene, besides the highly enhanced removal capacity toward heavy metal ions on $CaCO_3$ only. Synergistic effects occurred with the composite samples and the pollutants. Different from the well reported nZVI sample, the prepared samples were in the range of micron size and exhibited good cost performances from the stances of preparation and preservation and application.

Supplementary Information The online version contains supplementary material available at https://doi.org/10.1007/s11356-021-17899-0.

Authors contribution Yanhui Hu: writing—original draft, investigation, methodology. Weijian Gu: visualization, formal analysis. Huimin Hu: methodology. Xuewei Li: writing—review and editing, methodology. Qiwu Zhang: conceptualization, supervision, resources.

Funding This study was financially supported by the National Key Research and Development Program of China (Project No. 2019YFC1805600; 2019YFC1805601).

Declarations

Conflict of interest The authors declare no competing interests.

Ethical approval The authors declare that the current manuscript is original and complete, not a part of any other study, it is not submitted in any other place for publication and results are truly presented without fabrication.

Consent to participate Not applicable.

Consent to publish All the authors have approved the submission and agreed for the publication.

Data availability Data and all the other relevant material will be available for the editorial office at any stage for non-commercial purpose.

References

Balaz P, Achimovicova M, Balaz M, Billik P, Cherkezova-Zheleva Z, Criado JM, Delogu F, Dutkova E, Gaffet E, Gotor FJ, Kumar R, Mitov I, Rojac T, Senna M, Streletskii A, Wieczorek-Ciurowa K (2013) Hallmarks of mechanochemistry: from nanoparticles to technology. Chem Soc Rev 42(18):7571–7637

Beyer MK, Clausen-Schaumann H (2005) Mechanochemistry: the mechanical activation of covalent bonds. Chem Rev 105(8):2921–2948

Chatterjee S, Lim S, Woo SH (2010) Removal of reactive black 5 by zero-valent iron modified with various surfactants. Chem Eng J 160(1):27–32

Duan X, Sun H, Kang J, Wang Y, Indrawirawan S, Wang S (2015) Insights into heterogeneous catalysis of persulfate activation on dimensional-structured nanocarbons. Acs Catal 5(8):4629–4636

Fu F, Dionysiou DD, Liu H (2014) The use of zero-valent iron for groundwater remediation and wastewater treatment: a review. J Hazard Mater 267:194–205

Gong K, Hu Q, Yao L, Li M, Sun D, Shao Q, Qiu B, Guo Z (2018) Ultrasonic pretreated sludge derived stable magnetic active carbon for Cr(VI) removal from wastewater. Acs Sustain Chem Eng 6(6):7283–7291

Gu W, Zhang Q, Qu J, Li Z, Hu H, Liu Y, Li Y, Ai Z (2019) Formation of active zero-valent iron by simple co-grinding with $CaCO_3$ to protect fresh active surface for efficient removal of hexavalent chromium. Appl Surf Sci 490:81–88

Hidouri M, Bouzouita K, Kooli F, Khattech I (2003) Thermal behaviour of magnesium-containing fluorapatite. Mater Chem Phys 80(2):496–505

Hu H, Li X, Huang P, Zhang Q, Yuan W (2017) Efficient removal of copper from wastewater by using mechanically activated calcium carbonate. J Environ Manage 203:1–7

Hu H, Zhang Q, Yuan W, Li Z, Zhao Y, Gu W (2019) Efficient Pb removal through the formations of (basic) carbonate precipitates from different sources during wet stirred ball milling with $CaCO_3$. Sci Total Environ 664:53–59

Huot J, Ravnsbæk DB, Zhang J, Cuevas F, Latroche M, Jensen TR (2013) Mechanochemical synthesis of hydrogen storage materials. Prog Mater Sci 58(1):30–75

Jabeen H, Chandra V, Jung S, Lee JW, Kim KS, Kim SB (2011) Enhanced Cr(VI) removal using iron nanoparticle decorated graphene. Nanoscale 3(9):3583

James SL, Adams CJ, Bolm C, Braga D, Collier P, Friš IT, Grepioni F, Harris KDM, Hyett G, Jones W, Krebs A, Mack J, Maini L, Orpen AG, Parkin IP, Shearouse WC, Steed JW, Waddell DC (2011) Mechanochemistry: opportunities for new and cleaner synthesis. Chem Soc Rev 41:413–447

Jeon J, Kim M (2019) CO_2 storage and $CaCO_3$ production using seawater and an alkali industrial by-product. Chem Eng J 378:122180

Jioui I, Dânoun K, Solhy A, Jouiad M, Zahouily M, Essaid B, Len C, Fihri A (2016) Modified fluorapatite as highly efficient catalyst for the synthesis of chalcones via Claisen-Schmidt condensation reaction. J Ind Eng Chem 39:218–225

Kong L, Ruan Y, Zheng Q, Su M, Diao Z, Chen D, Hou LA, Chang X, Shih K (2020) Uranium extraction using hydroxyapatite recovered from phosphorus containing wastewater. J Hazard Mater 382:120784

Lawrinenko M, Wang Z, Horton R, Mendivelso-Perez D, Smith EA, Webster TE, Laird DA, van Leeuwen JH (2016) Macroporous carbon supported zerovalent iron for remediation of trichloroethylene. Acs Sustain Chem Eng 5(2):1586–1593

Li X, Lei Z, Qu J, Hu H, Zhang Q (2017) Separation of copper from nickel in sulfate solutions by mechanochemical activation with $CaCO_3$. Sep Purif Technol 172:107–112

Li Y, He X, Hu H, Zhang T, Qu J, Zhang Q (2018) Enhanced phosphate removal from wastewater by using in situ generated fresh trivalent Fe composition through the interaction of Fe(II) on $CaCO_3$. J Environ Manage 221:38–44

Mandel S, Tas AC (2010) Brushite (CaHPO4·2H2O) to octacalcium phosphate (Ca8(HPO4) 2 (PO4)4·5H2O) transformation in DMEM solutions at 36.5 °C. Mater Sci Eng: C 30(2):245–254

Qin L, Gao X, Li Q (2018) Upcycling carbon dioxide to improve mechanical strength of Portland cement. J Clean Prod 196:726–738

Raman CD, Kanmani S (2016) Textile dye degradation using nano zero valent iron: A review. J Environ Manage 177:341–355

Sheng G, Shao X, Li Y, Li J, Dong H, Cheng W, Gao X, Huang Y (2014) Enhanced removal of Uranium(VI) by nanoscale zerovalent iron supported on na–bentonite and an investigation of mechanism. J Phys Chem A 118(16):2952–2958

Toshima T, Hamai R, Tafu M, Takemura Y, Fujita S, Chohji T, Tanda S, Li S, Qin GW (2018) Morphology control of brushite prepared by aqueous solution synthesis. J Asian Ceram Soc 2(1):52–56

Vilardi G, Mpouras T, Dermatas D, Verdone N, Polydera A, Di Palma L (2018) Nanomaterials application for heavy metals recovery from polluted water: the combination of nano zero-valent iron and carbon nanotubes. Competitive adsorption non-linear modeling. Chemosphere 201:716–729

Wang M, Wu S, Guo J, Zhang X, Yang Y, Chen F, Zhu R (2019) Immobilization of cadmium by hydroxyapatite converted from microbial precipitated calcite. J Hazard Mater 366:684–693

Xu C, Zhang B, Wang Y, Shao Q, Zhou W, Fan D, Bandstra JZ, Shi Z, Tratnyek PG (2016) Effects of sulfidation, magnetization, and oxygenation on azo dye reduction by zerovalent iron. Environ Sci Technol 50(21):11879–11887

Xu C, Zhu L, Wang X, Lin S, Chen Y (2014) Fast and highly efficient removal of chromate from aqueous solution using nanoscale zerovalent iron/activated carbon (NZVI/AC). Water Air Soil Pollut 225(2)

Yang GCC, Lee H (2005) Chemical reduction of nitrate by nanosized iron: kinetics and pathways. Water Res 39(5):884–894

Yang Z, Ma X, Shan C, Guan X, Zhang W, Lv L, Pan B (2019) Activation of zero-valent iron through ball-milling synthesis of hybrid $Fe0/Fe_3O_4/FeCl_2$ microcomposite for enhanced nitrobenzene reduction. J Hazard Mater 368:698–704